Contribution from the Department of Chemistry,
Louisiana State University, Baton Rouge, Louisiana 70803-1804

Synthesis of a Binucleating Tetratertiary Phosphine Ligand System and the Structural Characterization of both Meso and Racemic Diastereomers of Ni_2Cl_4(eLTTP) (eLTTP = $(Et_2PCH_2CH_2)(Ph)PCH_2P(Ph)(CH_2CH_2PEt_2)$)

Scott A. Laneman, Frank R. Fronczek, and George G. Stanley*

Received October 27, 1988

The synthesis of the binucleating tetratertiary phosphine ligand system $(R_2PCH_2CH_2)(Ph)PCH_2P(Ph)(CH_2CH_2PR_2)$ (R = Et, Ph), LTTP, is described. The first synthetic step involves the reaction of $PhPH_2$ with $^1/_2$ equiv of CH_2Cl_2 and a 56% aqueous solution of KOH in DMF to produce $Ph(H)PCH_2P(H)Ph$ in 45–55% isolated yield. The second step utilizes the 2,2′-azobis(isobutyronitrile) (AIBN) free-radical-catalyzed addition of 2 equiv of $R_2PCH{=}CH_2$ (R = Et, Ph) with $Ph(H)PCH_2P(H)Ph$ in cyclohexane, which gives a nearly quantitative yield of LTTP. The reaction of 2 equiv of $NiCl_2{\cdot}6H_2O$ with the ethyl-substituted version of LTTP (eLTTP) in EtOH produces the bimetallic complex Ni_2Cl_4(eLTTP) (**2**). Both the meso- and racemic-diastereomeric forms of **2** readily crystallize from THF to produce THF-solvated crystals. The air-stable red-orange crystals are easily separated because the meso complex rapidly desolvates to give opaque crystals, while the racemic crystals retain the THF solvent and remain clear. Single-crystal X-ray structures of *meso*- and *rac*-Ni_2Cl_4(eLTTP) are presented. Crystal data for *rac*-Ni_2Cl_4(eLTTP): triclinic, $P\bar{1}$, a = 11.693 (6) Å, b = 13.830 (3) Å, c = 14.438 (3) Å, α = 111.87 (2)°, β = 110.95 (2)°, γ = 94.37 (2)°, V = 1963 (1) Å^3, Z = 2. Crystal data for *meso*-Ni_2Cl_4(eLTTP): monoclinic, space group $P2_1/c$, a = 16.919 (2) Å, b = 13.656 (2) Å, c = 15.966 (6) Å, β = 94.46 (2)°, V = 3678 (3) Å^3, Z = 4. Both structures have square-planar geometries with each half of the eLTTP ligand forming a five-membered bis(phosphine) chelate ring at each metal atom. The nickel atoms in both structures are well separated, with Ni···Ni distances of 5.417 (1) and 6.272 (1) Å for the racemic and meso complexes, respectively.

Introduction

The combination of a bis(phosphino)methane bridge with bis(phosphino)ethane chelating units in the hexatertiary phosphine $(Et_2PCH_2CH_2)_2PCH_2P(CH_2CH_2PEt_2)_2$, eHTP,[1] creates a unique

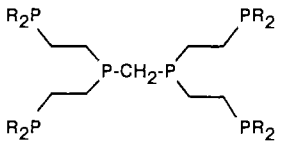

eHTP

merging of functionalities that are perfectly suited to the formation of bimetallic species.[2] We have also demonstrated that heterobimetallic systems can be readily prepared using eHTP.[3] Only in a single case has the formation of a monometallic system been observed when 2 equiv of a suitable transition-metal complex was treated with eHTP.[4]

One of our concerns with eHTP, however, is that the strongly bonding tridentate, bis-chelating nature of the ligand blocks three sites which can inhibit the reactivity of the metal center, particularly with low-valent group VIII metals that have typical coordination numbers of only 4 or 5. A simple approach to reducing some of the unfavorable steric factors in HTP is to conceptually backtrack and remove two of the $Et_2PCH_2CH_2$– chelate arms from HTP and prepare a new binucleating *tetra*-tertiary phosphine ligand of the general type $(R_2PCH_2CH_2)$-$(R)PCH_2P(R)(CH_2CH_2PR_2)$. This ligand would still have the bridging and chelating framework of HTP, yet provide a considerably more open environment about the metal centers for reactions to occur. A tetratertiary phosphine of this type is chiral at the two internal phosphorus atoms resulting in both racemic (*R*,*R* and *S*,*S*) and meso (*R*,*S*) diastereomers. We will subsequently refer to this general class of linear tetratertiary phosphine ligands as LTTP. We use the LTTP abbreviation to distinguish this more linear ligand from the tripodal tetratertiary phosphine

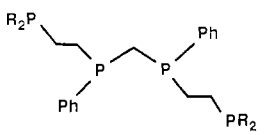

Racemic *R*,*R*- and *S*,*S*-LTTP

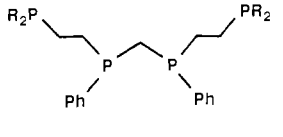

Meso *R*,*S*-LTTP

(R = Et, eLTTP; R = Ph, phLTTP)

ligand $P(CH_2CH_2PR_2)_3$ and the tridentate phosphine PhP-$(CH_2CH_2CH_2PPh_2)_2$, which is also commonly abbreviated as ttp. The chirality of this system is a desirable feature for promoting potential stereo- and enantioselective reactions, but will make for more difficult separations of the phosphine and/or bimetallic complexes.

The preparation of a ligand of the general type described above has been reported by Stelzer and coworkers who have synthesized the tetratertiary phosphine ligand system $(i\text{-}Pr_2PCH_2CH_2CH_2)(i\text{-}Pr)PCH_2P(i\text{-}Pr)(CH_2CH_2CH_2P\text{-}i\text{-}Pr_2)$.[5] A problem with their synthesis, however, is that the overall conversion from $Cl_2PCH_2PCl_2$ to the final tetratertiary phosphine is a 10–15% yield reaction.[6] Furthermore, they have not reported any transition-metal complexes based on this ligand. We would like to describe, therefore, an alternate higher yield synthetic route to the LTTP ligand $(R_2PCH_2CH_2)(Ph)PCH_2P(Ph)(CH_2CH_2PR_2)$ (R = Et, Ph), which was reported in a recent communication.[7] The preparation and structural characterization of both the meso and racemic diastereomers of Ni_2Cl_4(eLTTP) is also presented.

Experimental Section

General Data. All manipulations were carried out under inert atmosphere (N_2 or Ar) by using standard Schlenk or glovebox techniques unless stated otherwise. Solvents were distilled under inert atmosphere from the following drying agents: diethyl ether, hexane, THF (sodium/benzophenone); toluene (sodium); CH_2Cl_2 and acetonitrile (CaH_2); methanol and ethanol (magnesium). $PhPH_2$, Et_2PCl, $Ph_2PCH{=}CH_2$ (Strem Chemicals), $NiCl_2{\cdot}6H_2O$ (Alfa division of Morton Thiokol), 2,2′-azobis(isobutyronitrile) (Pfaltz & Bauer, Inc.), *N*,*N*-dimethylformamide (Mallinckrodt), cyclohexane, and $CH_2{=}CHMgBr$ (Aldrich) were used as received. $Et_2PCH{=}CH_2$ was prepared according to published procedures.[1] ^1H and ^{31}P NMR spectra were recorded on a Bruker AC-100, AC-200, or AM-400 spectrometer, IR spectra were run on a Perkin-Elmer 283B spectrometer, NMR simulations were done on a Bruker

(1) Askham, F. R.; Stanley, G. G.; Marques, E. C. *J. Am. Chem. Soc.* **1985**, *107*, 7423.
(2) (a) Laneman, S. A.; Stanley, G. G. *Inorg. Chem.* **1987**, *26*, 1177. (b) Askham, F. R.; Maverick, A. W.; Stanley, G. G. *Inorg. Chem.* **1987**, *26*, 3963. (c) Saum, S. E.; Stanley, G. G. *Polyhedron* **1987**, *6*, 1803. (d) Saum, S. E.; Askham, F. R.; Fronczek, F. R.; Stanley, G. G. *Organometallics* **1988**, *7*, 1409. (e) Saum, S. E.; Askham, F. R.; Fronczek, F. R.; Stanley, G. G. *Polyhedron* **1988**, *7*, 1785.
(3) Saum, S. E.; Askham, F. R.; Laneman, S. A.; Stanley, G. G. *Polyhedron*, submitted for publication.
(4) Askham, F. R.; Saum, S. E.; Stanley, G. G. *Organometallics* **1987**, *6*, 1370.
(5) Hietkamp, S.; Sommer, H.; Stelzer, O. *Chem. Ber.* **1984**, *117*, 3414.
(6) Hietkamp, S.; Sommer, H.; Stelzer, O. *Chem. Ber.* **1984**, *117*, 3400.
(7) Laneman, S. A.; Fronczek, F. R.; Stanley, G. G. *J. Am. Chem. Soc.* **1988**, *110*, 5585.

0020-1669/89/1328-1872$01.50/0

spectrometer using the simulation program PANIC, and elemental analyses were performed by Onedia Research Laboratories, Inc., Whitesboro, NY.

Synthesis of (Ph)(H)PCH$_2$P(H)(Ph). The procedure used for the preparation of (Ph)(H)PCH$_2$P(H)(Ph) was developed by Langhans and Stelzer.[8] $PhPH_2$ (31.52 g, 0.286 mol) and CH_2Cl_2 (12.18 g, 0.143 mol) were added to a flask with 330 mL of dimethylformamide (DMF) and cooled in an ice bath. Then, 43 mL of a 56% aqueous solution of KOH (56.1 g (1.0 mol) of KOH dissolved in 44 mL of H_2O) was added slowly over 1–1.5 h. As the addition proceeded, the solution gradually turned to a final deep yellow color with a yellow solid clinging to the sides of the flask. After the ice-cooled solution was stirred for 3–7 h, 218 mL of H_2O was added to the stirred solution, which generated some H_2 gas and turned the solution a cloudy white color. The resulting mixture was extracted with three 100-mL washes of pentane, which were combined and evaporated to produce a clear viscous liquid. This liquid was vacuum distilled (0.1 Torr) to give 7 g of a mixture of $PhPH_2$ and PhP(H)Me at 25–30 °C, and 15.4 g (46% yield) of the meso and racemic diastereomers of (Ph)(H)PCH$_2$P(H)(Ph), which distilled at 110–115 °C.

$^{31}P\{^1H\}$ NMR (C_6D_6, δ in ppm, H_3PO_4 reference): −56.3 and −57.6 (s). Stelzer reported yields of around 70% in his preparation, but we consistently obtained isolated yields of only 50 ± 5%.

eLTTP. $Et_2PCH{=}CH_2$ (3.84 g, 0.033 mol), (Ph)(H)PCH$_2$P(H)(Ph) (3.84 g, 0.017 mol), and 50 mL of cyclohexane were added to a Schlenk flask to which a degassed reflux condenser containing 0.0384 g of 2,2′-azobis(isobutyronitrile), AIBN, was carefully attached causing the AIBN to fall into the solution. The advantage of adding the AIBN this way is that it is fully degassed, a second flask does not have to be used, and it is not added to the solution until the heat is ready to be applied. An alternate procedure would be to initially place the AIBN in the reaction flask, degas, and then add the other components from a second flask via a cannula.

The reaction mixture was refluxed overnight and cooled, and the solvent was vacuum evaporated to give a viscous, clear, and colorless liquid. A short-head distillation column was placed on the flask, replacing the reflux condenser and a 0.1-Torr vacuum was applied to the system. The temperature was gradually raised to 170 °C, causing all impurities to distill away from the product. The residue contains 6.75 g (88% yield, typical isolated yields 75–90%) of eLTTP (purity > 98%).

Anal. Calcd for $C_{25}H_{40}P_4$: C, 64.66; H, 7.91. Found: C, 63.58; H, 7.91. $^{31}P\{^1H\}$ NMR (C_6D_6, δ in ppm, H_3PO_4 reference): diastereotopic internal phosphorus atoms, −26.2 (1 P, dd, J_{P-P} = 10.4 and 12.2 Hz) and −25.5 (1 P, dd, J_{P-P} = 10.2 and 12.1 Hz); external phosphorus atoms, −18.37 (1 P, dd, J_{P-P} = 10.3 and 12.5 Hz) and −18.31 (1 P, dd, J_{P-P} = 10.4 and 12.3 Hz). Computer-simulated coupling constants based on an AXX′A′ spin system: $J_{P_{int}-P_{ext}}$ = 22.5 Hz and $J_{P_{int}-P_{int}}$ = 109.5 Hz. ^1H NMR (C_6D_6, δ in ppm, TMS reference): 0.74–0.85 (m, P–CH$_2$–CH_3), 1.02–1.14 (m, P–CH_2–CH$_3$), 1.19–1.33, 1.33–1.46 (m, P–CH_2–CH_2–P), 1.72–1.89 (m, P–CH_2–P), 6.98–7.10 and 7.41–7.47 (m, Ph).

phLTTP. The procedure for preparing the all-phenylated LTTP (phLTTP) was the same as that described above for eLTTP except that one would use $Ph_2PCH{=}CH_2$. The workup following the reaction was, however, somewhat different. After the cyclohexane solvent was removed, the very viscous clear and colorless residue was taken up in 20 mL of Et_2O and placed in a −40 °C freezer overnight. A white microcrystalline powder formed on the sides of the flask that was mainly composed (ca. 80%) of the meso diastereomer (based on ^{31}P NMR). The total yield of the powder was 25–35%. The Et_2O was evaporated to give a very sticky solid from which the remaining impurities were removed by vacuum distillation up to 210 °C (0.1 Torr). The residue that remained was phLTTP (purity > 98%). Total isolated yield was 85–90%.

Anal. Calcd for $C_{41}H_{40}P_4$: C, 75.00; H, 6.10. Found: C, 75.22; H, 6.16. $^{31}P\{^1H\}$ NMR (C_6D_6, δ in ppm, H_3PO_4 reference): diastereotopic internal phosphorus atoms, −25.8 (1 P, dd, J_{P-P} = 13.3 and 17.0 Hz) and −25.2 (1 P, dd, J_{P-P} = 13.3 and 17.0 Hz); external phosphorus atoms, −11.9 (2 P, dd, J_{P-P} = 13.3 and 17.0 Hz). Computer-simulated coupling constants based on an AXX′A′ spin system: $J_{P_{int}-P_{ext}}$ = 29.9 Hz and $J_{P_{int}-P_{int}}$ = 107.6 Hz. ^1H NMR (MeOH-d_4, δ in ppm, TMS reference): 1.82–2.00, 2.01–2.13, 2.14–2.22 (m, P–CH_2–CH_2–P), 2.25 (t, P–CH_2–P), 7.12 and 7.37 (m, Ph).

Ni_2Cl_4(eLTTP). A 25-mL EtOH solution of eLTTP (2.00 g, 4.31 mmol) was added dropwise to a stirred clear green solution of $NiCl_2 \cdot 6H_2O$ (2.05 g, 8.62 mmol) in 25 mL of EtOH. The solution turned red as the addition proceeded, with an orange precipitate forming near the end of the reaction. After the mixture was stirred overnight, the orange precipitate was collected by filtration and washed with three 10-mL portions of cold EtOH to give 1.42 g (45% yield) of mainly *meso*-Ni_2Cl_4(eLTTP). The filtrate was evaporated to give 1.25 g (40% yield) of mainly *rac*-Ni_2Cl_4(eLTTP) for an overall isolated yield of 85%. Typical overall isolated yields for this reaction ranged from 80 to 95%.

The orange solid was dissolved in a minimum volume of CH_2Cl_2 and evaporated to dryness, yielding a red solid (this procedure enhanced the formation of crystals in the next step). The red solid was then dissolved in THF and allowed to gradually evaporate, giving rise to well-formed, medium to large crystals of *meso*- and *rac*-Ni_2Cl_4(eLTTP). The orange-red crystals were air-stable, but one crystal type quickly desolvated in air to give opaque crystals. Thus the two types of crystals can be easily separated under a microscope. An X-ray structural determination has identified the crystal type that desolvates as *meso*-Ni_2Cl_4(eLTTP), while the other is composed of *rac*-Ni_2Cl_4(eLTTP). On a larger scale, the red solid isolated from evaporation of a CH_2Cl_2 solution can be dissolved in a minimum quantity of THF and allowed to stand for 1 h. The reddish-orange precipitate that forms was *rac*-Ni_2Cl_4(eLTTP) with only a trace of the meso-diastereomer present.

***rac*-Ni_2Cl_4(eLTTP).** Anal. Calcd for $C_{25}H_{40}Cl_4Ni_2P_4$: C, 41.49; H, 5.57. Found: C, 42.14; H, 5.62. $^{31}P\{^1H\}$ NMR (CD_2Cl_2, δ in ppm, H_3PO_4 reference): external phosphorus (P_{ext}), 75.41 (1 P, dt, J_{P-P} = 69.0 and 3.9 Hz); internal phosphorus (P_{int}), 57.97 (1 P, dt, J_{P-P} = 69.0 and 3.9 Hz). ^1H NMR (MeOH-d_4, δ in ppm, TMS reference): see Table V.

***meso*-Ni_2Cl_4(eLTTP).** Anal. Calcd for $C_{25}H_{40}Cl_4Ni_2P_4$: C, 41.49; H, 5.57. Found: C, 40.87; H, 5.46. $^{31}P\{^1H\}$ NMR (CD_2Cl_2, δ in ppm, H_3PO_4 reference): P_{ext}, 74.28 (1 P, dt, J_{P-P} = 72.8 and 10.8 Hz); P_{int}, 58.32 (1 P, dt, J_{P-P} = 72.8 and 10.8 Hz). ^1H NMR (MeOH-d_4 δ in ppm, TMS reference): see Table V.

Removal of Nickel from *meso*- and *rac*-Ni_2Cl_4(eLTTP). A 0.186-g (0.257-mmol) sample of *rac*-Ni_2Cl_4(eLTTP) was added to 20 mL of H_2O with a 50-fold molar excess of NaCN present. The solution was refluxed for 2 h and allowed to cool. The free *rac*-eLTTP ligand was extracted from this yellow aqueous solution with three 15-mL portions of benzene. The yellow benzene solution was then passed through a short neutral alumina column, which separated the free eLTTP ligand from the yellow impurity which remained at the top of the column. The clear and colorless benzene solution containing eLTTP was evaporated to give 0.057 g (0.123 mmol) of *rac*-eLTTP (45% isolated yield). The same procedure was used for *meso*-Ni_2Cl_4(eLTTP) with similar yields.

X-ray Crystallography. Data were collected on an Enraf-Nonius CAD4 diffractometer at room temperature by using Mo Kα radiation and a graphite-crystal monochromator by the $\theta/2\theta$ scan technique using variable scanning rates. Crystal data and experimental details are listed in Table I. Data reduction included corrections for background, Lorentz, and polarization effects, as well as an empirical absorption correction based on ψ scans of reflections near χ = 90°. Structure solving was done by using the Enraf-Nonius Structure Determination Package on a MicroVAX II computing system. The one set of crystals that tended to desolvate was mounted in a capillary with a small amount of THF. Both crystals had a small amount of decay (3–7%) in the standard reflections, and a decay correction was applied to both data sets.

Both structures were solved by using the MULTAN direct-methods program set and refined by using full-matrix least-squares refinement and were found to have disordered THF solvent molecules lying on a crystallographic inversion center. Although we were able to model the disorder, the THF molecules are poorly defined, particularly so in the meso system. The racemic structure had disordered ethyl groups on the external phosphorus atoms that were successfully modeled. All disordered

Table I. Crystallographic Data for *meso*- and *rac*-Ni_2Cl_4(eLTTP)·*x*THF

	meso	racemic
formula	$Ni_2Cl_4P_4O_{1.5}C_{31}H_{52}$	$Ni_2Cl_4P_4OC_{29}H_{48}$
fw	831.86	795.83
space group	$P\bar{1}$ (No. 2)	$P2_1/c$ (No. 14)
a, Å	11.693 (6)	16.919 (2)
b, Å	13.830 (3)	13.656 (2)
c, Å	14.438 (3)	15.966 (6)
α, deg	111.87 (2)	90.00
β, deg	110.95 (2)	94.46 (2)
γ, deg	94.37 (2)	90.00
V, Å^3	1963 (1)	3678 (3)
Z	2	4
d_{calc}, g/mL	1.34	1.44
μ(Mo Kα), cm^{-1}	14.2	15.16
temp, °C	21	22
radiation; λ, Å	Mo Kα; 0.710 73	Mo Kα; 0.710 73
$R(F_o)$	0.058	0.062
$R_w(F_o)$	0.084	0.086
min transmissn coeff	0.8141	0.9498

(8) Langhans, K. P.; Stelzer, O. *Chem. Ber.* **1987**, *120*, 1707.

Scheme I

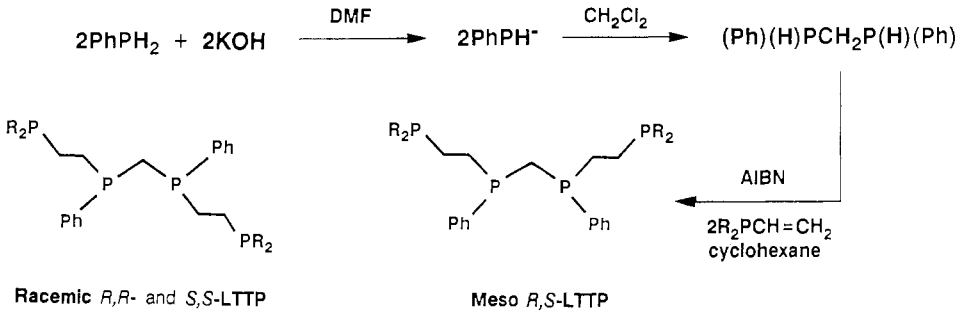

Table II. Positional Parameters for *meso*-Ni_2Cl_4(eLTTP)·1.5THF

atom	*x*	*y*	*z*	*B*,[a] Å^2
Ni1	0.2835 (1)	0.08911 (8)	0.77115 (8)	3.85 (3)
Ni2	0.4903 (1)	0.40464 (8)	1.27041 (8)	3.54 (3)
Cl1	0.2177 (3)	−0.0456 (2)	0.6082 (2)	7.08 (9)
Cl2	0.2872 (3)	−0.0126 (2)	0.8588 (2)	5.17 (7)
Cl3	0.6305 (2)	0.5518 (2)	1.3996 (2)	5.18 (7)
Cl4	0.3717 (3)	0.4892 (2)	1.1859 (2)	5.73 (8)
P1	0.3484 (2)	0.2303 (2)	0.9226 (2)	3.59 (6)
P2	0.2849 (3)	0.1956 (2)	0.6949 (2)	5.13 (8)
P3	0.3547 (2)	0.2564 (2)	1.1549 (2)	3.56 (6)
P4	0.5921 (2)	0.3126 (2)	1.3490 (2)	3.57 (6)
C′	0.2673 (8)	0.2294 (7)	1.0115 (6)	4.0 (2)
C11	0.3157 (9)	0.3473 (6)	0.8931 (7)	4.6 (3)
C12	0.355 (1)	0.3367 (7)	0.7994 (7)	5.1 (3)
C31	0.4234 (8)	0.1429 (6)	1.1577 (6)	3.8 (2)
C32	0.4993 (9)	0.1714 (6)	1.2821 (7)	4.3 (3)
C21	0.373 (1)	0.1755 (9)	0.6106 (9)	9.9 (4)
C22	0.513 (1)	0.171 (1)	0.682 (1)	14.2 (6)
C23	0.117 (1)	0.189 (1)	0.606 (1)	10.8 (5)
C24	0.084 (2)	0.263 (1)	0.575 (2)	16.2 (7)
C41	0.7428 (8)	0.2984 (7)	1.3406 (7)	4.6 (3)
C42	0.849 (1)	0.3993 (8)	1.406 (1)	6.9 (4)
C43	0.621 (1)	0.3639 (8)	1.4937 (7)	5.3 (3)
C44	0.679 (1)	0.2927 (9)	1.5492 (8)	8.3 (4)
C1P	0.5203 (8)	0.2622 (6)	0.9986 (6)	3.5 (2)
C2P	0.5807 (9)	0.1786 (7)	0.9776 (7)	4.5 (3)
C3P	0.7121 (9)	0.2008 (7)	1.0282 (7)	5.0 (3)
C4P	0.7821 (9)	0.3090 (8)	1.0995 (8)	5.7 (3)
C5P	0.721 (1)	0.3903 (7)	1.1197 (8)	6.1 (3)
C6P	0.5877 (9)	0.3673 (7)	1.0695 (7)	4.8 (3)
C7P	0.2263 (8)	0.2398 (6)	1.1946 (6)	3.9 (2)
C8P	0.2328 (9)	0.3154 (8)	1.2945 (7)	4.9 (3)
C9P	0.136 (1)	0.3000 (8)	1.3254 (8)	5.9 (3)
C10P	0.0339 (9)	0.2132 (8)	1.2605 (8)	5.4 (3)
C11P	0.0252 (9)	0.1384 (8)	1.1585 (7)	5.5 (3)
C12P	0.1217 (8)	0.1521 (8)	1.1267 (7)	4.9 (3)
C1S	0.220 (2)	0.946 (2)	0.197 (1)	10.6 (6)*
C1S′	0.235 (7)	0.879 (6)	0.215 (5)	10 (2)*
C2S	0.223 (2)	1.002 (2)	0.306 (2)	10.8 (7)*
C2S′	0.192 (5)	0.914 (4)	0.319 (4)	11 (2)*
C3S	0.117 (2)	0.962 (2)	0.321 (2)	7.8 (7)*
C3S′	0.044 (3)	0.915 (3)	0.228 (3)	12 (1)*
C4S	0.026 (2)	0.843 (2)	0.208 (2)	18.1 (19)*
C5S	0.119 (2)	0.878 (2)	0.151 (2)	12.2 (8)*
C5S′	0.162 (6)	0.807 (5)	0.224 (5)	14 (2)*
C6S	0.991 (6)	0.495 (5)	0.917 (4)	10 (2)*
C7S	0.939 (4)	0.492 (4)	0.999 (4)	8 (1)*
C8S	1.025 (4)	0.447 (3)	1.034 (3)	7 (1)*
C9S	0.968 (5)	0.596 (4)	1.071 (4)	9 (1)*
C10S	1.034 (5)	0.447 (4)	0.882 (4)	8 (1)*

[a] Starred values indicate atoms were isotropically refined. Values for anisotropically refined atoms are given in the form of the isotropic equivalent displacement parameter defined as $(4/3)[a^2\beta(1,1) + b^2\beta(2,2) + c^2\beta(3,3) + ab(\cos\gamma)\beta(1,2) + ac(\cos\beta)\beta(1,3) + bc(\cos\alpha)\beta(2,3)]$.

Table III. Positional Parameters for *rac*-Ni_2Cl_4(eLTTP)·THF

atom	*x*	*y*	*z*	*B*,[a] Å^2
Ni1	0.84885 (6)	0.19989 (8)	0.67459 (6)	3.92 (2)
Ni2	0.74388 (7)	−0.09454 (8)	0.86442 (7)	4.72 (3)
Cl1	0.9089 (2)	0.3401 (2)	0.7014 (2)	6.75 (7)
Cl2	0.7296 (1)	0.2646 (2)	0.6525 (2)	5.79 (6)
Cl3	0.8037 (2)	−0.1909 (2)	0.9573 (2)	9.96 (9)
Cl4	0.7348 (2)	−0.2035 (2)	0.7613 (2)	6.54 (6)
P1	0.8015 (1)	0.0583 (2)	0.6446 (1)	3.97 (5)
P2	0.9636 (1)	0.1310 (2)	0.6872 (2)	5.11 (6)
P3	0.6830 (1)	0.0109 (2)	0.7849 (1)	4.21 (5)
P4	0.7439 (2)	0.0128 (2)	0.9622 (2)	6.17 (7)
C′	0.7025 (5)	0.0207 (6)	0.6725 (5)	4.4 (2)
C11	0.8734 (6)	−0.0354 (7)	0.6858 (6)	6.1 (2)
C12	0.9552 (5)	0.0006 (7)	0.6605 (7)	6.3 (3)
C31	0.6964 (6)	0.1340 (6)	0.8307 (6)	5.8 (2)
C32	0.6866 (6)	0.1218 (6)	0.9268 (6)	5.6 (2)
C21	1.0367 (6)	0.1788 (9)	0.6198 (6)	7.1 (3)
C22	1.0070 (7)	0.182 (1)	0.5277 (7)	8.4 (3)
C23	1.0104 (6)	0.141 (1)	0.7972 (7)	11.4 (4)
C24	1.0847 (9)	0.143 (2)	0.8109 (9)	16.9 (6)
C41	0.730 (1)	−0.028 (2)	1.069 (1)	7.9 (6)*
C41′	0.676 (1)	−0.022 (1)	1.053 (1)	5.7 (4)*
C42	0.667 (2)	−0.087 (2)	1.066 (2)	11.1 (8)*
C42′	0.604 (1)	−0.060 (2)	1.033 (2)	9.1 (7)*
C43	0.851 (1)	0.080 (2)	0.984 (1)	7.4 (5)*
C43′	0.830 (1)	0.038 (2)	1.019 (1)	6.3 (5)*
C44	0.920 (2)	0.024 (2)	0.986 (2)	9.4 (7)*
C44′	0.884 (1)	0.091 (2)	0.951 (1)	7.0 (5)*
C1P	0.7912 (5)	0.0426 (6)	0.5308 (5)	4.2 (2)
C2P	0.7986 (6)	0.1218 (7)	0.4785 (6)	5.6 (2)
C3P	0.7961 (6)	0.1119 (8)	0.3917 (6)	6.9 (3)
C4P	0.7810 (5)	0.0186 (9)	0.3583 (6)	6.9 (3)
C5P	0.7696 (5)	−0.0638 (8)	0.4083 (6)	5.9 (2)
C6P	0.7751 (5)	−0.0523 (7)	0.4969 (6)	5.2 (2)
C7P	0.5757 (5)	−0.0105 (8)	0.7777 (6)	5.6 (2)
C8P	0.5483 (6)	−0.1007 (8)	0.8078 (7)	7.2 (3)
C9P	0.4655 (6)	−0.120 (1)	0.8046 (8)	9.6 (4)
C10P	0.4154 (7)	−0.043 (1)	0.7667 (7)	11.0 (5)
C11P	0.4418 (7)	0.046 (1)	0.7364 (8)	10.4 (4)
C12P	0.5246 (6)	0.061 (1)	0.7423 (6)	8.0 (3)
C1S	0.516 (1)	0.344 (2)	0.061 (1)	11.4 (6)*
C2S	0.431 (1)	0.348 (2)	0.023 (1)	11.2 (6)*
C3S	0.437 (1)	0.340 (2)	0.060 (1)	10.3 (5)*
C4S	0.510 (2)	0.269 (2)	−0.072 (2)	14.7 (8)*
C5S	0.571 (1)	0.320 (2)	0.003 (2)	13.4 (7)*
C6S	0.537 (2)	0.397 (3)	0.038 (3)	8 (1)*
C7S	0.475 (2)	0.296 (3)	0.065 (2)	7.4 (9)*
C8S	0.540 (3)	0.253 (4)	0.016 (4)	13 (2)*
C9S	0.534 (2)	0.311 (3)	−0.078 (3)	7.9 (9)*
C10S	0.571 (3)	0.368 (4)	−0.035 (3)	10 (1)*

[a] Starred values indicate atoms were refined isotropically. Values for anisotropically refined atoms are given in the form of the isotropic equivalent displacement parameter defined as $(4/3)[a^2\beta(1,1) + b^2\beta(2,2) + c^2\beta(3,3) + ab(\cos\gamma)\beta(1,2) + ac(\cos\beta)\beta(1,3) + bc(\cos\alpha)\beta(2,3)]$.

atoms were refined with isotropic thermal parameters. Because of the disorder problems, hydrogen atoms were not included in the final structure factor calculation. Positional parameters for the meso and racemic structures are listed in Tables II and III. Full tables of crystal and data collection parameters, anisotropic thermal parameters, bond distances and angles, and observed and calculated structure factors for both structures are included in supplementary material.

Results and Discussion

LTTP Ligand System. The synthetic procedure for preparing the LTTP ligand $(R_2PCH_2CH_2)(Ph)PCH_2P(Ph)(CH_2CH_2PR_2)$ (R = Et, Ph) is shown in Scheme I and involves the building of

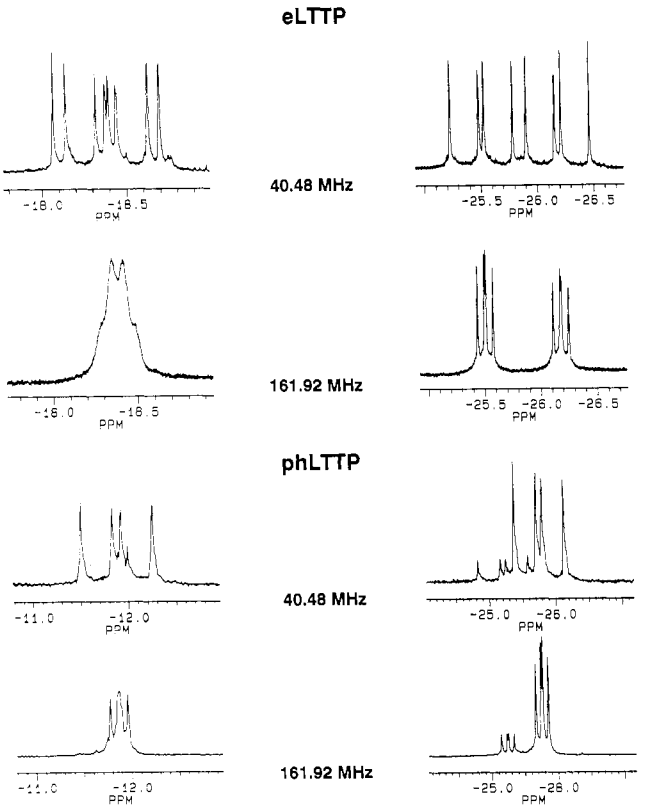

Figure 1. $^{31}P\{^1H\}$ NMR spectra of eLTTP and phLTTP at the two different field strengths indicated. The lower field is equivalent to a ^1H resonance frequency of 100 MHz, while the higher field corresponds to 400 MHz.

the central bis(phosphino)methane unit from the reaction of KP(H)Ph with CH_2Cl_2. The Ph(H)PCH_2P(H)Ph species thus produced is isolated and then treated with 2 equiv of R_2P-(CH=CH_2) under AIBN free-radical-catalyzed conditions[9] to produce LTTP. The use of ethylene-linked terminal phosphines in LTTP simplifies the synthetic procedure and gives higher yields of the final tetratertiary phosphine (88–92% yield based on Ph-(H)PCH_2P(H)Ph, 39–43% yield based on starting $PhPH_2$) relative to the use of propylene-linked groups in Stelzer's synthesis.[5] The presence of phenyl groups on the central P–CH_2–P bridge is a designed feature of this ligand and should allow more ready crystallizations of transition-metal complexes. Although we have prepared the all-phenyl-substituted LTTP (phLTTP) ligand, our primary interest is in the ethyl-substituted LTTP (eLTTP) ligand because the electron-rich alkylated terminal phosphines will coordinate strongly to transition-metal centers and be far more effective at inhibiting ligand dissociation and dimer fragmentation processes.

Interestingly, the reaction of KPHPh with CH_2Cl_2 has been reported by Issleib and Jacob *not* to yield any PhHPPCH_2PHPh, but only polymethylene and the bisphosphine PhHPPHPh.[10] An important consideration in their procedure, however, was that the CH_2Cl_2 was added *to* a suspension of KPHPh. We have previously observed in the synthesis of Et_2P(CH=CH_2) that the order of addition of the reactants is critical,[1] and the same is true in this reaction as well. We have found that the slow addition of KPHPh to CH_2Cl_2 in THF at 0 °C produces the desired bis(phosphino)methane PhHPPCH_2PHPh in ca. 25% yield along with PhPHMe (30%), $PhPH_2$ (15%), and the two cyclic phosphines $(PhP)_4CH_2$ (20%) and $CH_2(PhP)_4CH_2$ (10%).[11] Although PhHPPCH_2PHPh can be separated by a combination of crystallization and subsequent distillation, a superior preparation of PhHPPCH_2PHPh was recently reported by Stelzer through the reaction of $PhPH_2$, CH_2Cl_2, and KOH in DMSO/H_2O or DMF/H_2O, and this is the procedure we are currently using.[8]

Figure 1 shows expanded $^{31}P\{^1H\}$ NMR spectra of phLTTP and eLTTP at 40.48 MHz (100-MHz ^1H equivalent) and 161.92 MHz (400-MHz ^1H equivalent) resonant frequencies. The 40.48-MHz spectra, in particular, are the result of careful shimming of the NMR spectrometer and do not use any line broadening. The rather dramatic change in the appearance of the ^{31}P resonances with field strength turns out to be very deceptive. The P–P couplings and spin systems, for example, are identical for each sample at the two field strengths. Simulations using an AXX'A' spin system produce a simple doublet–doublet pattern for the internal and external phosphorus atoms with the following coupling constants: $J_{P_{int}-P_{ext}}$ = 22.5 Hz and $J_{P_{int}-P_{int}}$ = 109.5 Hz for eLTTP; $J_{P_{int}-P_{ext}}$ = 29.9 Hz and $J_{P_{int}-P_{int}}$ = 107.6 Hz for phLTTP. The complexity of the P_{ext} resonance in eLTTP arises from the overlapping of two separate doublet of doublets that are offset by ca. 0.1 ppm, one from each diastereomeric form of LTTP. This can be seen in phLTTP where the meso diastereomer predominates and the doublet–doublet nature of the resonance for the P_{ext} atoms can be more clearly seen.

The reason that the higher field spectra appear to be different is the greater line width of the resonances combined with the larger Hz/ppm, which compresses the couplings together when plotted on a ppm scale. The combination of two slightly chemically shifted overlapping doublet–doublet patterns for the P_{ext} atoms in eLTTP with greater line widths in the higher field spectrum gives rise to broad, ill-defined resonances. The 161.92-MHz spectrum does, however, clearly separate and show the relative proportions of the meso and racemic diastereomers of LTTP. Both meso and racemic diastereomers of eLTTP and phLTTP are produced in equal quantities from the synthetic procedure and are not thermally interconvertible up to a temperature of 200 °C. We have not attempted any experiments to see whether photolysis can effect interconversions between the two diastereomers.

Ni_2Cl_4(eLTTP). The meso and racemic diastereomers of LTTP are powerful binucleating ligands that can both bridge and chelate two metal centers, but they will form complexes that have different overall orientations of the phosphines about the two metal centers as shown for idealized M–M bonded dimer systems.

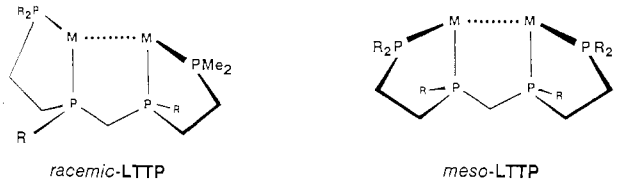

We have not, as yet, directly separated the two eLTTP ligand diastereomers (vide infra), although the all-phenyl-substituted version, phLTTP, does selectively crystallize the meso over the racemic diastereomer, allowing a relatively simple partitioning of the two diastereomers. The ethyl-substituted ligand, eLTTP, which we are primarily interested in, will require more sophisticated column or HPLC techniques to separate its meso and racemic forms, and we are currently exploring various separation procedures. Another strategy is to treat the diastereomeric eLTTP mixture with metal complexes to produce bimetallic M_2(eLTTP) systems and then take advantage of the differences between the *rac*-M_2(eLTTP) and *meso*-M_2(eLTTP) orientations and polarities to effect separation by simple column chromatography or by fractional crystallization.

The reaction of 2 equiv of $NiCl_2 \cdot 6H_2O$ with eLTTP in EtOH produces Ni_2Cl_4(eLTTP) in nearly quantitative yield. The $^{31}P\{^1H\}$ NMR spectrum indicates the presence of both diastereomeric forms of Ni_2Cl_4(eLTTP) in roughly equal amounts. No upfield ^{31}P resonances are observed, consistent with the coordination of all phosphorus atoms to the nickel centers. Both the meso and racemic forms of Ni_2Cl_4(eLTTP) crystallize from THF as large, well-shaped THF-solvated orange-red and red-orange crystals with different morphologies. One set of these air-stable crystals,

(9) DuBois, D. L.; Hyers, W. H.; Meek, D. W. *J. Chem. Soc., Dalton Trans.* **1975**, 1011.
(10) Issleib, K.; Jacob, D. *Chem. Ber.* **1961**, *94*, 107.
(11) Laneman, S. A.; Fronczek, F. R.; Stanley, G. G. *Phosphorus Sulfur*, in press.

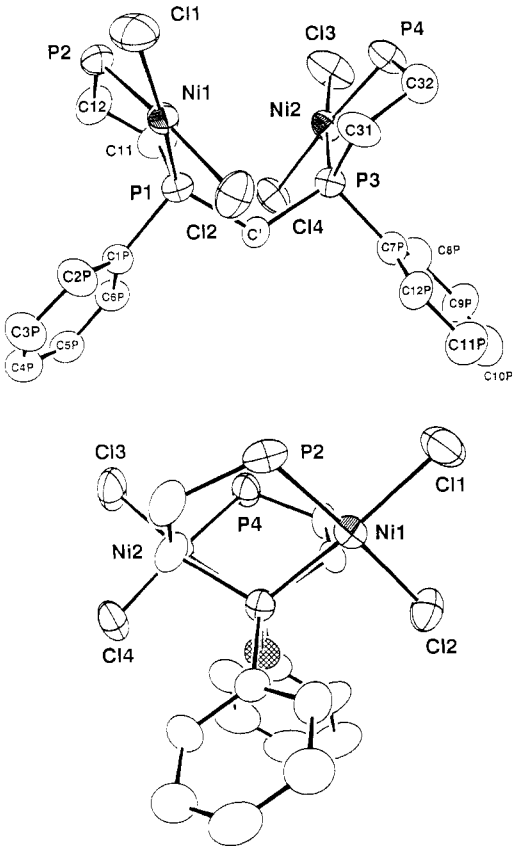

Figure 2. ORTEP plots of *rac*-Ni_2Cl_4(eLTTP) oriented parallel and perpendicular to the central P1···P3 vector to illustrate the rotational orientation. The ethyl groups on the external phosphorus atoms are removed for clarity. The central methylene group is hatched in the perpendicular view to highlight its position. Thermal ellipsoids are shown at the 33% probability level.

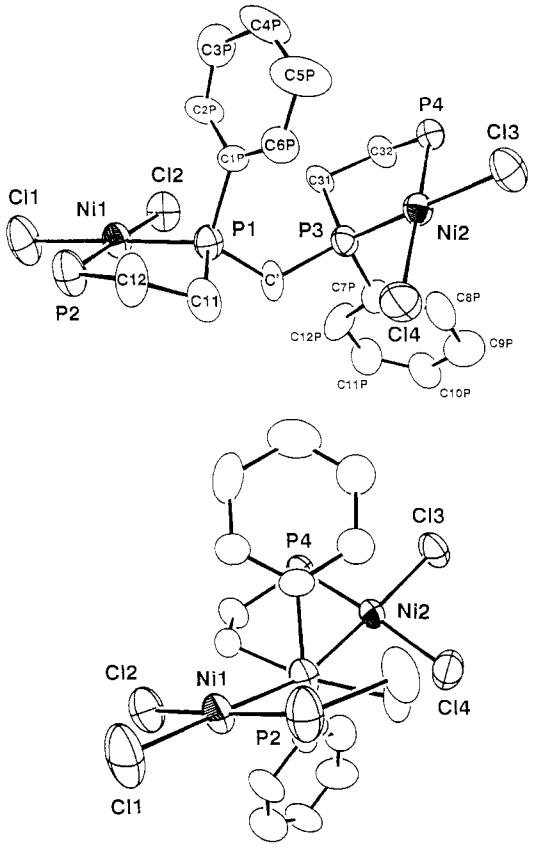

Figure 3. ORTEP plots of *meso*-Ni_2Cl_4(eLTTP) oriented parallel and perpendicular to the central P1···P3 vector to illustrate the rotational orientation. The ethyl groups on the external phosphorus atoms are removed for clarity. The central methylene group in the perpendicular view is oriented down as in Figure 2 and is hidden behind P2. Thermal ellipsoids are shown at the 33% probability level.

moreover, quickly loses the THF solvent of crystallization in air to turn opaque, while the other crystal type retains the THF solvent and remains clear, allowing easy manual separation of the two diastereomers. ^{31}P NMR spectra of the separated crystals show that they do indeed correspond to the two different diastereomers of Ni_2Cl_4(eLTTP). The two diastereomers can also be separated by column chromatography.

X-ray structural determinations on each type of crystal confirm that they are indeed the two different diastereomers of Ni_2Cl_4(eLTTP) with the crystals that readily lose THF containing the *meso*-eLTTP complex. ORTEP plots of views parallel and perpendicular to the central P1···P3 vector for the *rac*- and *meso*-Ni_2Cl_4(eLTTP) compounds are shown in Figures 2 and 3, respectively. Selected bond distances and angles for both structures are listed in Table IV. Since d^8 Ni(II) atoms generally do not form Ni–Ni bonds,[12] it was not surprising to find open-mode structures for each diastereomer. Both systems have square-planar environments about the nickel centers with the eLTTP ligand coordinating in the expected bridging/chelating manner. The local coordination geometry about each nickel center is very similar to that seen in the structure on the monometallic complex $NiCl_2$(dppe) (dppe = 1,2-bis(diphenylphosphino)ethane).[13] The structural discussion will concentrate, therefore, on the rotational orientations found in these bimetallic systems.

We will continue to make use of the syn and anti nomenclature previously used for the M_2(eHTP) complexes[2a,2d] to designate the general rotational orientation of each half of the complex with respect to the central methylene bridge hydrogen atoms. Syn will, therefore, refer to when a metal atom is on the same side of the eLTTP ligand as the central methylene group hydrogen atoms, while anti will indicate that the metal atom is on the opposite side.

Table IV. Selected Bond Distances (Å) and Angles (deg) for *meso*- and *rac*-Ni_2Cl_4(eLTTP)

	meso	racemic
Ni1–Ni2	6.272 (1)	5.417 (1)
Ni1–Cl1	2.195 (2)	2.194 (2)
Ni1–Cl2	2.208 (2)	2.205 (2)
Ni1–P1	2.139 (2)	2.134 (2)
Ni1—P2	2.144 (2)	2.153 (2)
Ni2–Cl3	2.187 (2)	2.173 (2)
Ni2–Cl4	2.209 (2)	2.215 (2)
Ni2–P3	2.136 (2)	2.131 (2)
Ni2–P4	2.160 (2)	2.141 (2)
P1–C′	1.852 (7)	1.838 (6)
P3–C′	1.824 (7)	1.854 (6)
Cl1–Ni1–Cl2	95.17 (8)	94.90 (8)
Cl1–Ni1–P1	175.55 (9)	174.26 (8)
Cl1–Ni1–P2	88.06 (9)	87.86 (8)
Cl2–Ni1–P1	90.27 (8)	90.25 (7)
Cl2–Ni1–P2	176.75 (9)	175.63 (8)
P1–Ni1–P2	86.50 (8)	86.86 (8)
Cl3–Ni2–Cl4	94.13 (8)	95.89 (9)
Cl3–Ni2–P3	175.07 (9)	173.48 (9)
Cl3–Ni2–P4	89.79 (8)	86.74 (9)
Cl4–Ni2–P3	89.58 (8)	90.46 (8)
Cl4–Ni2–P4	175.30 (9)	175.9 (1)
P3–Ni2–P4	86.37 (7)	86.84 (8)
Ni1–P1–C′	115.0 (2)	122.1 (2)
Ni2–P3–C′	121.5 (2)	120.7 (2)
P1–C′–P3	121.7 (4)	119.3 (3)

[a] Numbers in parentheses are estimated standard deviations in the least significant digits.

(12) There are a few Ni(II) dimer systems that have short Ni–Ni separations (around 2.4–2.6 Å) which can be described as Ni=Ni double bonds. Cf.: (a) Fackler, J. P., Jr. *Prog. Inorg. Chem.* **1976**, *21*, 55. (b) Corbett, M.; Hoskins, B. F.; McLeod, N. J. *Aust. J. Chem.* **1975**, *28*, 2377.

(13) Spek, A. L.; Van Eijck, B. P.; Jans, R. J. F.; Van Koten, G. *Acta Crystallogr., Sect. C: Cryst. Struct. Commun.* **1987**, *C43*, 1878.

Table V. ^1H NMR Data for *meso*- and *rac*-Ni_2Cl_4(eLTTP)

	meso			racemic		
proton	δ, ppm	$J(^1H-^1H)$, Hz	$J(^1H-^{31}P)$, Hz	δ, ppm	$J(^1H-^1H)$, Hz	$J(^1H-^{31}P)$, Hz
P-CH_2-CH_3	1.01	7.7 (t)	20.0 (d)	1.16	7.8 (t)	20.0 (d)
	1.07	7.7 (t)	17.2 (d)	1.36	7.8 (t)	17.2 (d)
P-CH_2-CH_3	1.35	7.4 (q)	15.6 (d)	1.61	7.7 (q)	14.8 (d)
	1.46	7.8 (q)	9.2 (d)	2.13	7.8 (q)	10.0 (d)
	1.77	1.2 (d)	11.2 (d)	2.26	7.7 (q)	8.8 (d)
		7.8 (q)		2.23	7.8 (q)	11.2 (d)
	1.97	8.0 (q)	10.0 (d)			
P-CH_2-CH_2-P	1.57	2.0 (d)	12.0 (d)	1.91	2.0 (d)	11.6 (d)
		6.8 (d)			7.0 (d)	
		14.8 (d)			13.5 (d)	
	1.68	7.0 (d)	6.4 (d)	2.05	1.9 (d)	10.8 (d)
		8.0 (d)			7.0 (d)	
		15.0 (d)			15.1 (d)	
	2.67	2.6 (d)	15.6 (d)	2.87	2.0 (d)	14.8 (d)
		6.4 (d)			6.5 (d)	
		12.8 (d)			15.5 (d)	
	2.74	2.0 (d)	15.6 (d)	2.99	2.0 (d)	14.0 (d)
		6.2 (d)			6.5 (d)	
		13.0 (d)			15.5 (d)	
P-CH_2-P	3.21	14.2 (d)	11.6 (t)	3.27		14.8 (t)
	3.64	14.2 (d)	14.0 (t)			
P-*Ph*	7.66	3.3 (t)		7.54	1.9 (d)	*a*
					3.3 (t)	
	8.82	3.0 (d)	12.0 (d)	8.37	1.8 (d)	12.0 (d)
		5.7 (d)			8.2 (d)	

[a] J_{P-H} was present but unmeasurable.

The ultimate anti-anti conformer would be what we refer to as a closed-mode geometry, and it could accommodate a M-M bond.

The structure of *rac*-Ni_2Cl_4(eLTTP) is, therefore, in an anti-anti rotational conformation with the two nickel atoms symmetrically splayed open, very similar to the structures seen for *rac*-$Rh_2Cl_2(CO)_2$(eLTTP)[7] and the eHTP complexes M_2Cl_2(eHTP)$^{2+}$ (M = Pd, Pt)[2c,14] and $M_2(CO)_6$(eHTP) (M = Cr, Mo, W).[2d] The Ni1-P1···P3-Ni2 torsional angle for the racemic complex is 106° with a Ni-Ni separation of 5.417 (1) Å. *rac*-$Rh_2Cl_2(CO)_2$(eLTTP), for example, has a Rh-P1···P1′-Rh′ torsional angle of 123° and a Rh-Rh distance of 5.813 (2) Å.[7] This can also be compared to the M_2Cl_2(eHTP)$^{2+}$ (M = Pd, Pt) complexes, which have considerably smaller M-P1···P1′-M′ torsional angles of 58° for Pd and 62° for Pt. We will not compare the racemic complex to Ni_2Cl_2(eHTP)$^{2+}$ because of the different rotational conformers that each adopts. The M-M separations further reflect the partially closed-mode configurations in the M_2Cl_2(eHTP)$^{2+}$ complexes with Pd-Pd = 4.4217 (8) Å and Pt-Pt = 4.6707 (9) Å.[13]

The smaller M-P1···P1′-M′ torsional angles in the M_2Cl_2(eHTP)$^{2+}$ complexes might lead one to believe that there are also smaller intramolecular steric interactions in the eHTP binuclear systems relative to Ni_2Cl_4(eLTTP). This would be disturbing because the eLTTP ligand was designed to be less bulky than eHTP. In order to properly assess the intramolecular steric effects, it is far more appropriate to compare the P-CH_2-P and average M-P-CH_2 angles. *rac*-Ni_2Cl_4(eLTTP), for example, has P-C-H_2-P and average Ni-P-CH_2 angles of 119.3 (3) and 118°, respectively. This can be contrasted to the larger P-CH_2-P and average M-P-CH_2 angles in the eHTP complexes M_2Cl_2(eHTP)$^{2+}$: 126.6 (4) and 121° (Pd); 129.7 (9) and 121° (Pt).

In contrast with the racemic diastereomer, *meso*-Ni_2Cl_4(eLTTP) has the syn-anti rotational conformation with a considerably larger Ni1-P1···P3-Ni2 torsional angle of 160° and Ni-Ni separation of 6.272 (1) Å (Figure 3, Table IV). The metal-ligand bond distances and angles are essentially the same as seen in the racemic system. The major difference between the two structures is the rotational orientation about the central methylene bridge. The syn-anti conformation seen in *meso*-Ni_2Cl_4(eLTTP) is inherently somewhat asymmetric relative to the symmetrically splayed structure for the racemic complex. This is most apparent in the two Ni-P_{int}-C′ bond angles, which have fairly different values in the meso system: Ni1-P1-C′ = 115.0 (2)° and Ni2-P3-C′ = 121.5 (2)°. In a syn-anti structure half of the bimetallic complex experiences a more crowded steric environment, which, for the meso complex, is the Ni2 side. A completely analogous effect is seen in the Ni_2Cl_2(eHTP)$^{2+}$ complexes.[2a,13] This allows the M-P_{int}-C′ bond angle on the *less* crowded side of the complex to relax to a greater extent relative to the angle on the more sterically encumbered half of the complex.

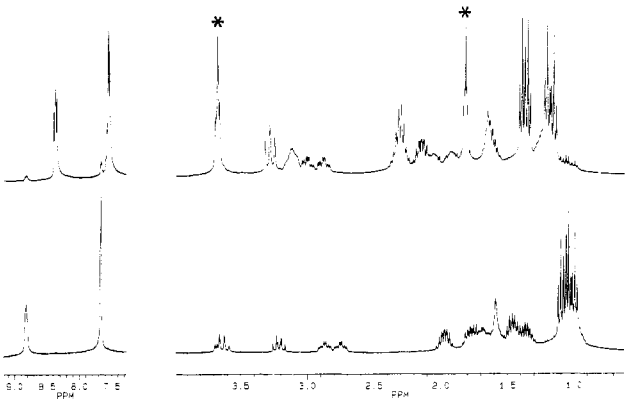

Figure 4. ^1H NMR spectra of *rac*- (top) and *meso*-Ni_2Cl_4(eLTTP) (bottom). Peaks marked with a star in the racemic spectrum are due to THF, which is present as a solvent of crystallization. A small amount of the meso complex is present in the racemic complex; this is responsible for the low-intensity resonances at 1.0 ppm and in the phenyl region.

The ^1H NMR spectra for *rac*- and *meso*-Ni_2Cl_4(eLTTP) are shown in Figure 4. We have used two-dimensional ^1H *J*-correlated experiments to identify the various resonances and separate the $^1H-^1H$ and $^1H-^{31}P$ coupling constants for these resonances. We have found that the *J*-correlated method is exceptionally well suited for organophosphine systems where $^1H-^1H$ and $^1H-^{31}P$ coupling constants occur simultaneously. Our detailed assignments and the coupling constants for these spectra are listed in Table V. One item of interest is the resonance for the central methylene group, which is a triplet (δ = 3.27 ppm) in the racemic complex

(14) Saum, S. E.; Laneman, S. A.; Stanley, G. G. *Inorg. Chem.*, submitted for publication.
(15) (a) Allen, D. L.; Gibson, V. C.; Green, M. L. H.; Skinner, J. F.; Bashkin, J.; Grebenik, P. D. *J. Chem. Soc., Chem. Commun.* **1983**, 895. (b) Schenck, T. G.; Downes, J. M.; Milne, C. R. C.; Mackenzie, P. B.; Boucher, H.; Whelan, J.; Bosnich, B. *Inorg. Chem.* **1985**, *24*, 2334.

but appears as two separate pseudoquartet (doublets of triplets) patterns (δ = 3.21 and 3.64 ppm) in the meso system (Figure 4). For the racemic system, assuming an averaged symmetric structure in solution, the central methylene bridge protons are expected to be equivalent and only have coupling to the two equivalent P_{int} phosphorus atoms. The P-CH_2-P protons in the meso complex, on the other hand, are inequivalent and should give rise to two separate resonances that will show both ^1H-^1H and ^1H-^{31}P coupling constants, and this is exactly what is observed.

Isolation of Pure *meso*- and *rac*-eLTTP Ligands. The ability to easily separate the meso and racemic forms of Ni_2Cl_4(eLTTP) suggested that the nickel complex could provide a vehicle for isolating each diastereomer if the ligand could be displaced from the nickel centers. Fortunately, cyanide anion has been successfully used in the past to displace phosphine ligands from Ni(II) complexes.[15] Refluxing *rac*- or *meso*-Ni_2Cl_4(eLTTP) in an aqueous solution of NaCN displaces eLTTP from the nickel atoms to produce $Ni(CN)_4^{2-}$. eLTTP is readily extracted from the aqueous solution with benzene, which, after column chromatography and evaporation, gives the pure eLTTP ligand in 45% isolated yield.

The ability to separate the racemic and meso diastereomers of eLTTP will considerably simplify our work in preparing, characterizing, and studying the reactivity of M_2(eLTTP) complexes, particularly since *rac*- and *meso*-M_2(eLTTP) complexes of other metals (e.g., Rh, Co) are not always as easy to separate as Ni_2Cl_4(eLTTP). Although we are still working on a direct chromatographic separation of the two diastereomers of eLTTP, the nickel route is currently satisfactory and several grams of each pure eLTTP diastereomer has been isolated.

Acknowledgment. We thank the National Science Foundation (Grant CHE-86-13089) for supporting this research.

Supplementary Material Available: Figure S-1 (^{31}P NMR spectra for *rac*- and *meso*-Ni_2Cl_4(eLTTP)) and Tables S-I-S-VII (crystal and data collection parameters, all bond distances and angles, and anisotropic thermal parameters) (11 pages); Tables S-VIII and S-IX (observed and calculated structure factors) (28 pages). Ordering information is given on any current masthead page.

Contribution from the Departments of Chemistry, Washington University, St. Louis, Missouri 63130, and Louisiana State University, Baton Rouge, Louisiana 70803-1804

Thermal and Photochemical Reactivity of Group VI Open-Mode Bimetallic Complexes Based on a Binucleating Hexaphosphine Ligand System. Crystallographic Characterization of a Novel Ditungsten Heptacarbonyl Pentaphosphine Compound

Suzanne E. Saum,[1a] Frank R. Fronczek,[1b] Scott A. Laneman,[1b] and George G. Stanley*,[1b]

Received May 10, 1988

The thermal and photochemical reactivities of an isomorphous series of group VI bimetallic complexes, $M_2(CO)_6$(eHTP) (M = Cr, Mo, W; eHTP = $(Et_2PCH_2CH_2)_2PCH_2P(CH_2CH_2PEt_2)_2$), are reported. Thermally, the pure complexes are stable to refluxing xylene for extended periods of time. In the synthesis of $W_2(CO)_6$(eHTP), however, the occasional in situ formation of tungsten metal causes a partial fragmentation of the eHTP ligand. Single-crystal X-ray data for the isolated yellow complex from this fragmentation shows that it crystallizes in the acentric monoclinic space group *Pc* with a = 15.072 (4) Å, b = 8.007 (2) Å, c = 15.104 (7) Å, β = 102.8 (1)°, V = 1778 (2) Å^3, and Z = 2. The structure was refined to R = 0.029 and R_w = 0.039 by using 2281 unique data with $F_o^2 > 3\sigma(F_o^2)$. The structure reveals a ditungsten heptacarbonyl compound with an unusual pentaphosphine ligand derived from eHTP with the formula $W_2(CO)_7(C_{19}H_{43}P_5)$. The original eHTP ligand has lost one of the four $Et_2PCH_2CH_2$- arms, and the resulting unsaturated phosphorus atom has formed a new P-C bond (with loss of H) to the starred carbon atom on a $Et_2PC^*H_2CH_2$- arm from the other half of eHTP. This generates a multicycle pentaphosphine ligand that forms four- and five-membered chelate rings with one $W(CO)_3$ moiety and a single standard five-membered bis(phosphine) chelate with the other $W(CO)_4$ unit. The photolysis of the binuclear $M_2(CO)_6$(eHTP) (M = Cr, Mo, W) compounds in CH_2Cl_2 proceeds to give two distinct types of products: *mer,mer*-Cr_2Cl_6(eHTP) and $M_2Cl_4(CO)_4$(eHTP) (M = Mo, W). $Cr_2(CO)_6$(eHTP) is extremely photoreactive toward CH_2Cl_2, with the chlorination reaction forming Cr_2Cl_6(eHTP) proceeding in good yield and driven by even ambient laboratory fluorescent lighting. The Mo and W systems are considerably less photoreactive, with mercury lamp irradiation taking 4-6 days to produce two isomeric forms of the open-mode 7-coordinate $M_2Cl_4(CO)_4$(eHTP) (M = Mo, W) species.

Introduction

The hexatertiary phosphine ligand $(Et_2PCH_2CH_2)_2PCH_2P(CH_2CH_2PEt_2)_2$, eHTP, was designed to be a powerful binucleating ligand for lower valent transition-metal centers, and so far, every time we have reacted it with 2 equiv of a simple mononuclear metal halide, we have obtained a binuclear system. Our efforts have been directed at understanding the coordination chemistry of this polyphosphine ligand and its dynamic properties.[2-5] Recently we reported the synthesis and characterization of a homoleptic series of binuclear group VI systems based on eHTP, $M_2(CO)_6$(eHTP) (M = Cr, Mo, W).[6] These bimetallic compounds have an open-mode type eHTP conformation with M-M separations of ca. 6.3-6.5 Å. A schematic representation of these complexes is as follows:

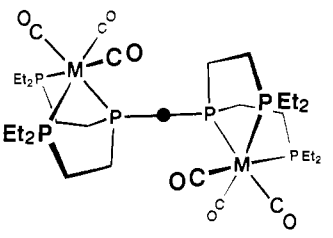

It is somewhat difficult to come up with a proper nomenclature for identifying the various rotamers for the eHTP ligand, but we have used the syn and anti notations in describing our nickel system[3] and will continue with this nomenclature. Syn will, therefore, refer to the case where a metal atom is on the same side of the eHTP ligand as the central methylene group hydrogen atoms, while anti will indicate that the metal atom is on the opposite side. Although the solid-state structures of the $M_2(CO)_6$(eHTP) complexes have an anti-anti orientation of the metal

(1) (a) Washington University. (b) LSU.
(2) Askham, F. R.; Marques, E. C.; Stanley, G. G. *J. Am. Chem. Soc.* **1985**, *107*, 7423.
(3) Laneman, S. A.; Stanley, G. G. *Inorg. Chem.* **1987**, *26*, 1177.
(4) Saum, S. E.; Stanley, G. G. *Polyhedron* **1987**, *6*, 1803.
(5) Askham, F. R.; Maverick, A. W.; Stanley, G. G. *Inorg. Chem.* **1987**, *26*, 3963.
(6) Saum, S. E.; Askham, F. R.; Fronczek, F.; Stanley, G. G. *Organometallics* **1988**, *7*, 1409.

0020-1669/89/1328-1878$01.50/0